INTERACTIVE CONTROL ENGINEERING
Principles and Applications

Volume 20 Motion Control, Robotics, and Autonomous Systems

CHAPTER 3

Drone Taxi Simulator for Load Feedforward and Wind Estimation Between Buildings

Pages 54–78

Edited by John D. Hedengren

How to cite this chapter. "Drone Taxi Simulator for Load Feedforward and Wind Estimation Between Buildings," in *Motion Control, Robotics, and Autonomous Systems*, John D. Hedengren, Ed., vol. 20 of *Interactive Control Engineering: Principles and Applications*. Advanced Process Solutions, LLC, 2026, ch. 3, pp. 54–78.

The page numbers in this file are those of the printed volume.

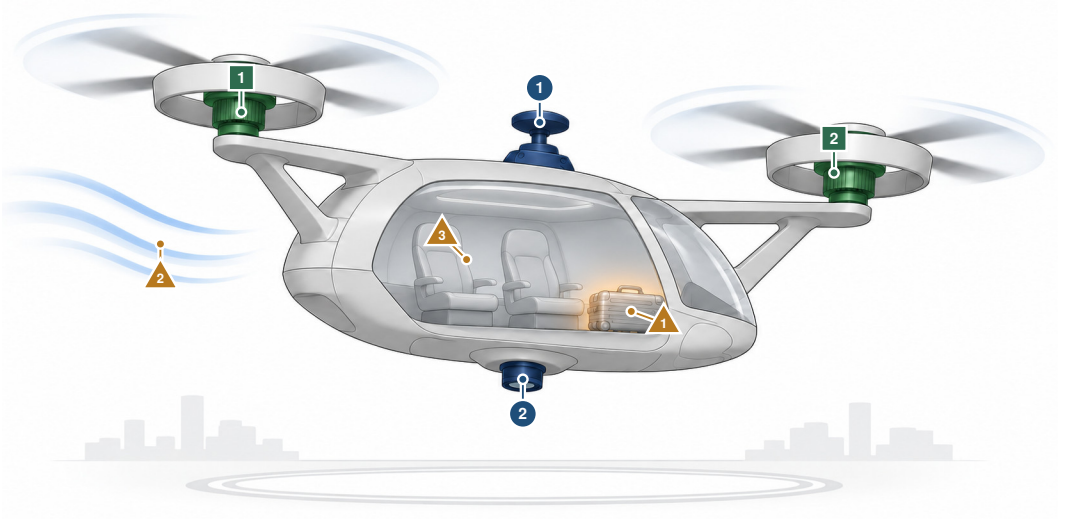
The app for this chapter
https://apmonitor.com/apps/drone-taxi/

The volume online: contents, other chapters and citation records
https://apmonitor.com/apps/books/v20-motion-robotics/#drone-taxi

Copyright © 2026 Advanced Process Solutions, LLC. All rights reserved. Produced by Advanced Process Solutions, LLC.

CHAPTER 3

Drone Taxi Simulator for Load Feedforward and Wind Estimation Between Buildings



The controller moves 1 the left rotor group, which lifts the taxi
2 the right rotor group: pushing harder on one side tilts the taxi

The controller reads 1 the navigation unit on the roof: position, height and tilt
2 the downward-looking sensor: height above the pad

What disturbs it 1 the suitcase on the sliding tray, which moves the balance point 2 the wind between the buildings
3 passengers boarding at each pad, who change the weight

Notice that the taxi has no wing: the two rotor groups carry its whole weight, and it leans to move sideways or to stand against the wind. Illustration, not to scale.

IN PLAIN TERMS Telling a Flying Taxi What It Carries

The main idea. A flying taxi with no wing is held up by its spinning rotors, and it moves sideways by leaning, pushing harder on one side than the other. A computer adjusts those pushes many times a second to keep it on its path.

The challenge. Every stop brings a new load, and the wind changes behind every building. A computer that only reacts to its own errors lets a heavy taxi lag and drift, so it helps to tell it the load and let it estimate the push of the wind.

Why it matters. A passenger flight has to land near the center of a small rooftop pad.

THREE WAYS TO READ THIS CHAPTER

Explore	9 min	the first page, the fact on the size of research quadrotors (Section 3.1), the history of the quadrotor (Section 3.2), the history of the disturbance observer (Section 3.4), the try-it segment and the fact on the graded route (Section 3.6), and the key points
Study	45 min	the whole chapter with its three pause points and the twelve exercises at its end
Practice	15 min	the first page, the results (Section 3.6), Technology in Practice (Section 3.7), Limitations (Section 3.8) and the open challenge

The control question A passenger multirotor meets a new load at every rooftop and a new wind behind every building. What is it worth to tell the flight controller the load, or to let it estimate the force it was not told about, rather than leave both to the integral terms?

Learning objectives

- Compute the mass, center of mass, trim and thrust margin of a loaded vehicle from its weight and balance and its battery charge.
- Predict from a force and a gain the error a loop keeps when it is not told about the force, and explain why the tilt error never decays.
- Separate the work of a weight feedforward from that of a gain scheduled on the mass.
- Compare an integral and a disturbance observer on a wind that changes along the route, including the cost of a faster observer.
- Explain what the dispatch, gate and go-around rules of the supervisor protect.

Prerequisites Sections 1.4.3, 1.4.4, 1.4.7, 1.6.2 and 1.6.4, with the loop-action convention of Section 1.3.

The app https://apmonitor.com/apps/drone-taxi/



See also Volume 3, Chapter 10 for a position loop that commands an attitude and Volume 3, Chapter 12 for the gravity feedforward of a load that changes along a route. Volume 5, Chapter 13 for an ocean current carried as an estimated state.

3.1 Introduction

A feedback loop learns about a disturbance only from the error that the disturbance has already caused. A heavier load, a shifted center of mass and a steady wind are forces that a controller could be told about or could estimate, yet a first course usually leaves each of them to the integral term. Motion control met the same limitation when a proportional position servo carrying an unknown load torque, such as friction or gravity, was shown to keep a steady and a transient error, and the disturbance observer was the answer [1]. Observer-based rejection has since spread across industrial sectors [2], and flight control was among the first applications of scheduling a controller on the measured operating condition [3].

The class of problem is broad. A crane lifting different containers, an elevator with a varying number of riders, a robot arm picking parts of unknown mass and a ship holding station in changing weather all carry a load that differs from one run to the next and meet an environment that changes with position or time. Each disturbance has a part known before the run, a part that can be inferred from the motion, and a remainder that only feedback can remove. Feedforward, scheduled gains and an observer are the three standard tools for the first two parts [2, 3].

An electric multirotor air taxi carries all three parts on one vehicle. It has no wing, so the rotors hold the whole weight at every instant, and it moves sideways only by tilting that thrust, which puts attitude inside the horizontal position loop of a cascade [4]. Among electric vertical takeoff and landing configurations the multirotor is the most efficient in hover [5], which suits short trips between rooftops, and short trips are where the load changes most often. Buildings shelter the air behind them and shed turbulent wakes [6], gaps between them channel the flow, and in simulated flight of a small unmanned helicopter the building wakes of an 8 kt wind changed its attitude by as much as 10° [7].

✦ DID YOU KNOW? Research Quadrotors Weighed a Few Kilograms

In 2007 the research groups working on quadrotors consistently chose vehicles of 0.3 to 4.0 kg [8]. A six-passenger quadrotor concept, flown in a piloted motion simulator in 2021, carries a payload of 1,200 pounds [9]. The two-seat vehicle of this chapter is 400 kg empty with a 220 kg payload rating.

The belief this plant is built to dislodge is that a well-tuned feedback loop has no need to know its load. In the application the same gains hold a light climb within 0.09 m of its reference and let

a heavy one fall 1.78 m behind, a suitcase at the end of the baggage tray leaves a standing tilt error of 2.46° that no attitude gain can remove, and an integral that has learned a wind keeps the vehicle leaning after the wind has gone. A transfer function drawn at one operating point shows none of this. Reviews of process control practice and of good practice in control teaching both favor experiments in which the behavior of a realistic plant, rather than algebra, decides the outcome [10, 11].

However, the value of each kind of knowledge is easy to state and hard to see, because it depends on how large the unknown force is against the loop gain and on how fast the force changes along the path. This chapter treats what a flight controller knows about its load and its wind as the experimental variable of a drone taxi simulator, and measures what each level of knowledge is worth on the same route. Cascaded multirotor control, gain scheduling, disturbance observers and jerk-limited references are all standard methods, and Section 1.4.3 sets out the first three on a cart. Section 3.2 follows the domain from helicopter stabilizers to passenger multirotors. Section 3.3 builds a nine-state planar vehicle whose rotor arms are taken about the true center of mass, with weight and balance set at boarding, a battery whose power limit sags at low charge, and a closed-form wind field attached to the buildings that the model and the scene share, each stated with its constants. Section 3.4 describes the three loops, the three levels of knowledge and the supervisor. Section 3.5 derives an error budget that predicts from a force and a gain how far each loop must stray to supply what it was not told, and separates feedforward from scheduling. Section 3.6 gives the measurements of ten cases and a graded route that isolate load, balance, wind, battery and approach one at a time, including the trade-off in observer bandwidth. Section 3.7 names the sensors, the motors and the weight and balance rules of a real multirotor, Section 3.8 states the limitations and Section 3.9 draws the results together.

3.2 Hover, City Wind and the Passenger Multirotor

Vertical flight has always been a control problem as much as a propulsion problem. A helicopter in hover is dynamically unstable, and the treatment of rotorcraft aeromechanics that covers its flight dynamics also supplies the momentum theory, figure of merit and rotor effects used in this chapter [12]. Helicopter control systems grew from simple mechanical stabilizing devices into automatic flight control systems that hold the aircraft for its pilot [13].

Multirotors took a different path. Several fixed-pitch rotors on a rigid frame need no swashplate, and attitude comes from the difference in thrust between rotors, which makes the vehicle mechanically simple and entirely dependent on its feedback loops. The history box below tells how the quadrotor became a research platform. The standard architecture places an attitude loop inside a position loop on inertial estimates [4], and the same vehicles now estimate the external force and moment acting on them from their own dynamics and inertial measurements, for collision detection and for flight in wind [14].

> ⧖ HISTORY **Four Rotors Waiting for Fast Electronics (1920s to 2007)**
>
> The first successful quadrotors flew in the 1920s, yet no practical quadrotor was built for decades, largely because four motors are hard to control at once with enough bandwidth. A crewed quadrotor of 1963 left ground effect, but it had no stability augmentation to lighten the pilot's work, so a steady hover was near impossible, and it stopped at the prototype. Faster microprocessors and micro-electro-mechanical inertial sensors later brought small radio-controlled quadrotors with stability augmentation. By 2007 the quadrotor was a popular research platform, simple to build and maintain and able to hover, with fixed-pitch rotors controlled by motor speed alone. Flight tests then showed that airspeed, angle of attack and airframe design add moments that disturb the attitude and thrust variations that disturb the altitude, effects a design made at hover does not anticipate [8].

The observer used by the third controller mode came from motion control, as the history box in Section 3.4 tells. Gain scheduling, the tool of the second mode, had its early examples in flight control and automotive engine control [3].

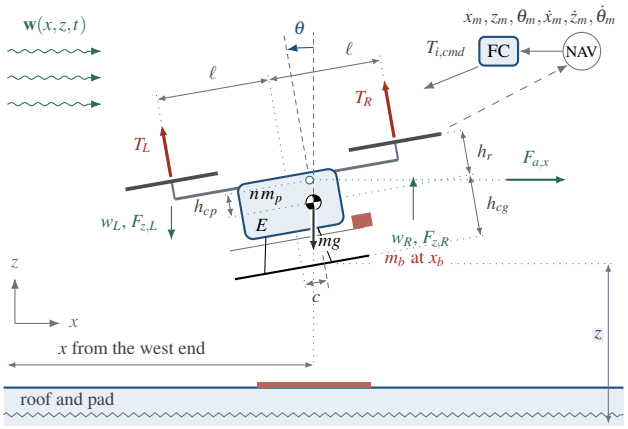


Figure 3.1 The planar air taxi as modeled, with the tilt drawn exaggerated. Two rotor groups at a distance ℓ either side of their centroid produce T_L and T_R along the body axis, a height h_r above the center of mass, which sits a distance c from the centroid set by the baggage m_b at x_b, with the n passengers of mass m_p on the centroid. The wind $\mathbf{w}$ drives a horizontal air force $F_{a,x}$ acting a height h_{cp} over the center of mass and a vertical drag $F_{z,i}$ at each group from its local vertical wind w_i. The skid height z is measured from the street below the break, and the navigation system NAV passes noisy states to the flight computer FC, which commands the group thrusts $T_{i,cmd}$ from the battery energy E.

Wind around buildings has its own literature. The flow around a single surface-mounted block separates and leaves a turbulent wake whose structure depends on the turbulence and shear of the approaching flow [6]. Rotorcraft flying through building wakes see large attitude disturbances [7], and the inability to fly well in adverse weather is among the obstacles listed for wider use of drones in cities [15].

Passenger air taxis carry these problems into commercial service. Of the three main electric configurations the multirotor is the most efficient in hover, the vectored-thrust jet in cruise, and lift-plus-cruise designs sit between [5]. Reviews of urban air mobility list certification and policy, traffic management and ground infrastructure among the questions still open [16], and the battery performance needed to electrify vertical takeoff and landing has been set out as a list of required metrics [17]. Comfort enters through the route. Studies of acceleration and jerk in ground transport vary too widely to fix one acceptable profile [18], so the comfort limits here are design choices, as are all the numerical targets of the application.

3.3 A Planar Air Taxi Among Rooftops

The vehicle belongs to the two-seat multirotor class, 400 kg empty with a 220 kg payload rating, and flies in the vertical plane of its route. The scene draws four rotors on each side, and the model lumps each side into one rotor group with one thrust acting a distance ℓ either side of the rotors' centroid. Horizontal position x points right, the height z of the landing skids above the street points up, and the tilt θ is measured counterclockwise, so a positive tilt leans the thrust toward $-x$. The geometry is shown in Figure 3.1.

Table 3.1 sorts every signal by its role. Nine states are integrated, the position and velocity in x and z, the tilt and its rate, the two group thrusts and the battery energy. The mass, center of mass and inertia change only when passengers or baggage move on a pad or the tray slides in flight, and the wind is a function of position and time.

Table 3.1 Variables, With Nominal Values From the Calm Hover of Case 1

Symbol	Role	Nominal	Range
z	CV, skid height	40 m	0–90 m
x	CV, horizontal position	28 m	0–400 m
θ	CV of the inner loop, tilt	0°	—
T	MV, total thrust	4.80 kN	0–8.4 kN
θ_{SP}	MV of the position loop	0°	±15°
ΔT	MV of the tilt loop, $T_R - T_L$	0 N	±4.05 kN
$\dot{x}, \dot{z}, \dot{\theta}$	states, rates	0	—
T_L, T_R	states, group thrusts	2.40 kN	0–4.2 kN
E	state, battery energy	19.2 kWh	0–24 kWh
n, m_p	DV, passengers, mass each	1, 80 kg	0–2, 50–120
m_b, x_b	DV, baggage and tray position	10 kg, 0	0–40, ±1.5 m
e_m	DV, load-sheet mass error	0 %	±30 %
U_0	DV, background wind at 50 m	0 m/s	±14 m/s
s_t	DV, turbulence scale	1	0–2
—	DV, gust front, push, bag slide	events	—

3.3.1 Rigid Body and Rotor Groups

The thrust points along the body axis, $(-\sin\theta, \cos\theta)$ in the earth frame, which gives the translational balance of Equation (3.1).

$$\begin{aligned} m\ddot{x} &= -T\sin\theta + F_{a,x} + F_p \\ m\ddot{z} &= T\cos\theta - mg + F_{a,z}, \qquad T = T_L + T_R \end{aligned} \tag{3.1}$$

where F_p is a push event of 600 N for 2 s. Tilt buys horizontal force and costs vertical force, and at 5° the vertical share of the thrust falls by 0.38 %. The pitch balance of Equation (3.2) takes each rotor arm from the actual center of mass.

$$I\ddot{\theta} = (\ell - c)\,T_R - (\ell + c)\,T_L + M_a \tag{3.2}$$

where c is the center of mass measured along the body axis from the rotors' centroid, positive toward the right group, and M_a is the aerodynamic moment. Setting $\ddot{\theta} = 0$ in still air gives the trim of a level hover, $T_R - T_L = cT/\ell \approx mgc/\ell$, so a center of mass off the centroid needs a standing difference in thrust. Each group follows its command through a first-order lag, $\tau_T \dot{T}_i = T_{i,cmd} - T_i$ for $i \in \{L, R\}$, and negative thrust is set to zero after each step.

3.3.2 Weight and Balance

The seats sit on the rotors' centroid and the baggage tray slides along the body axis, which gives the mass properties of Equation (3.3).

$$\begin{aligned} m &= m_e + nm_p + m_b, \qquad c = \frac{m_b x_b}{m} \\ I &= I_e + m_e c^2 + nm_p\left(r_p^2 + c^2\right) + m_b\,(x_b - c)^2 \end{aligned} \tag{3.3}$$

Passengers change the mass and the inertia, and baggage also moves the center of mass. A 40 kg suitcase at $x_b = -1.5$ m with one passenger gives $m = 520$ kg, $c = -11.5$ cm and a level-hover trim of −294 N. Boarding happens only on a pad. Each passenger walks between the roof door and the cabin in 2.2 s, successive passengers start 0.9 s apart, the baggage takes 1.2 s, and the mass changes as each passenger crosses the cabin door. In flight the mass is constant, while the tray can slide.

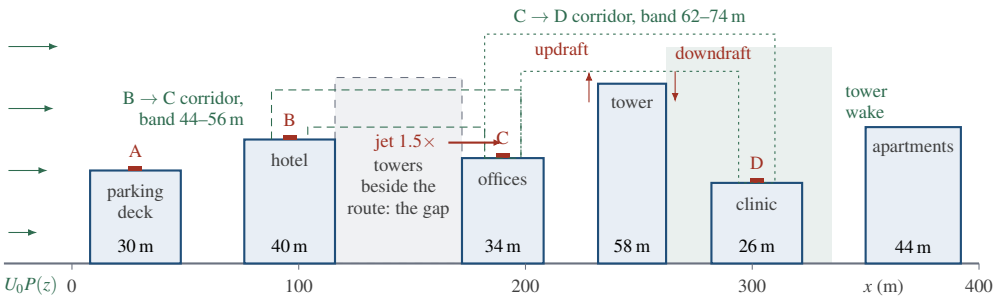


Figure 3.2 The street, with the lengths to one scale and the heights to a larger one, the pads A to D and the buildings' heights. The two towers beside the route over the plaza make the gap, whose channeled flow leaves as a jet over pad C when the wind blows toward $+x$, and the 58 m tower sheds a wake over pad D with an updraft at its windward roof edge and a downdraft behind its leeward one. The dashed outlines are the corridors of the two legs of the graded route, a shaft 16 m wide over each pad and a cruise band 12 m deep centered 10 m above the highest roof between the pads. The arrows at the left show the background profile $U_0P(z)$.

3.3.3 Air Loads

Drag follows the airspeed relative to the local wind, with a different area on each axis, as shown in Equation (3.4).

$$\begin{aligned} v_{r,x} &= \dot{x} - u, \qquad v_{r,i} = \dot{z} + \dot{\theta}\, r_i - w_i \\ F_{a,x} &= -\tfrac{1}{2}\rho\, C_d A_x V_r\, v_{r,x} \\ F_{z,i} &= -\tfrac{1}{2}\rho\, \tfrac{1}{2} C_d A_z \sqrt{v_{r,x}^2 + v_{r,i}^2}\; v_{r,i} \\ M_a &= r_R F_{z,R} + r_L F_{z,L} - h_{cp} F_{a,x} \end{aligned} \tag{3.4}$$

where u is the horizontal wind at the center of mass, w_i the vertical wind at rotor group i, $r_{R,L} = (\pm\ell - c)\cos\theta$ the horizontal lever arms of the groups, $V_r = [v_{r,x}^2 + (\dot{z} - \bar{w})^2]^{1/2}$ with $\bar{w} = (w_L + w_R)/2$, and $F_{a,z} = F_{z,L} + F_{z,R}$. Splitting the vertical area between the groups lets a roof-edge updraft under one group pitch the vehicle, and raising the horizontal drag h_{cp} above the center of mass leans the vehicle downwind. A vehicle drifting with the wind feels no force. The vertical wind is sampled at each group's rotor plane, a height h_r above a center of mass that is itself h_{cg} above the skids.

3.3.4 The City and Its Wind

Six buildings stand along a 400 m street, and four carry a pad of half-width 3 m, as shown in Figure 3.2. They are a parking deck from 8 to 48 m, 30 m tall with pad A at 28 m, a hotel from 76 to 116 m, 40 m tall with pad B at 96 m, offices from 172 to 208 m, 34 m tall with pad C at 190 m, a tower from 232 to 262 m, 58 m tall, a clinic from 282 to 322 m, 26 m tall with pad D at 302 m, and apartments from 350 to 392 m, 44 m tall. Between B and C an open plaza from 116 to 172 m is flanked by two 60 m towers that stand beside the route rather than on it, and they make the gap.

The wind at a point is the background speed $U(t)$ at the reference height of 50 m, shaped by a

Table 3.2 Wind-Field Features for a Wind Toward $+x$. H Is the Building Height, d the Distance Downwind of Its Leeward Face, a the Distance Upwind of Its Windward Face, s the Distance Along the Roof, $S(v) = 1/(1+\mathrm{e}^{-v})$, $B(v) = \mathrm{e}^{-v^2}$, and Lengths Inside S and B Are in Meters

Feature	Where	Contribution
lee shelter	$0 < d \le 6H$	$f_s = 1 - k_s\,\mathrm{e}^{-d/(L_w H)}\,S(h_w - z)\,R$ below the shear layer $h_w = H[1.1 + 0.15\min(d/H, 2)]$, with $k_s = 1.05$ and $L_w = 2.5$
lee turbulence	$0 < d \le 6H$	$f_t^2 \mathrel{+}= \{0.24\,\mathrm{e}^{-d/(3.2H)}\,R\,[0.6\,S(h_w - z) + B((z - h_w)/0.22H)]\}^2$
leeward downdraft	$0 < d \le 6H$	$f_w \mathrel{-}= 0.35\,e_k P(H)\,\mathrm{e}^{-d/(0.6H)}\,B((z - 0.95H)/0.38H)$
windward stagnation	$0 < a \le 1.5H$	$f_s = 1 - 0.55\,\mathrm{e}^{-a/(0.45H)}\,S((0.85H - z)/1.5)$
windward updraft	$0 < a \le 1.5H$	$f_w \mathrel{+}= 0.45\,e_k P(H)\,\mathrm{e}^{-a/(0.35H)}\,B((z - 0.92H)/0.3H)$
roof bubble	on the roof	$f_s = 1 - 0.65\min(1, e_k)\,\mathrm{e}^{-s/(0.8H)}\,b$ and $f_t^2 \mathrel{+}= [0.22\min(1, e_k)\,\mathrm{e}^{-s/(0.8H)}\,b]^2$, with $b = S((1.2H - z)/0.8)\,S((z - H + 0.5)/0.3)$
roof speed-up, roll-over	on the roof	speed $\times\,[1 + 0.12\min(1, e_k)\,B((z - 1.32H)/0.35H)]$, and $f_w \mathrel{+}= 0.3\,e_k P(H)\,\mathrm{e}^{-s/(0.3H)}\,B((z - 1.12H)/0.25H)$
gap	116–172 m, below 60 m	weight $g = S(a_g/2.5)\,E\,S((60 - z)/2.5)$ with $E = 1$ inside and $\mathrm{e}^{-d_g/20}$ past the exit, and $f_t^2 \mathrel{+}= (0.12g)^2$
combination	everywhere	f_s is the smallest shelter factor, $f_u = (1 - g) f_s\,\mathrm{speed} + g\,k_{gap}$, $f_w \leftarrow f_w(1 - 0.7g)$, and f_t^2 starts at 0.06^2

a_g and d_g are the distances past the gap entrance and exit, $R = 1 - S(a_g/2.5)S((60 - z)/2.5)$ removes the wake of a building upwind of the entrance once the channeled flow has replaced it, and e_k is the exposure of building k, the upstream shelter and gap factor evaluated 2 m upwind of its windward roof edge and floored at 0.1, so a low roof in the wake of a tall one has weak edge flows of its own.

power-law profile and by closed-form features attached to the buildings, as shown in Equation (3.5).

$$
\begin{aligned}
u &= U P(z_c) f_u(x, z_c) + \sigma n_u(t) \\
w_i &= |U| f_w(x_i, z_i) + 0.6\,\sigma n_w(t) \\
\sigma &= s_t |U| P(z_c) f_t(x, z_c) \\
P(z) &= (\max(z, 2\,\mathrm{m})/50\,\mathrm{m})^{\alpha} \\
U &= U_0 \big[1 + 0.08\sin(2\pi t/T_1 + \phi_1) \\
&\qquad + 0.05\sin(2\pi t/T_2 + \phi_2)\big] + U_g
\end{aligned}
\tag{3.5}
$$

where $z_c = z + h_{cg}$ is the height of the center of mass, f_u the horizontal speed as a fraction of the free stream, f_w the vertical speed as a fraction of $|U|$, and f_t the turbulence intensity. The slow variation has periods $T_1 = 23\,\mathrm{s}$ and $T_2 = 9.1\,\mathrm{s}$, with phases ϕ_1 and ϕ_2 drawn once per run from the scenario seed. The turbulence signals n_u and n_w are first-order colored noise of unit standard deviation with correlation times of 1.2 and 0.6 s, drawn on the controller clock and held over each control step so that the Runge-Kutta stages see a smooth right-hand side. A gust front adds $U_g = \frac{1}{2} A_g [1 - \cos(2\pi(t - t_0)/D_g)]$ for $t_0 \le t \le t_0 + D_g$, with $A_g = 6\,\mathrm{m/s}$ and $D_g = 6\,\mathrm{s}$ unless a case says otherwise. The features that make up f_u, f_w and f_t are listed in Table 3.2. The field mirrors itself when the wind reverses, and the scene draws its arrows and shaded zones from the same functions, so the picture and the flight cannot disagree. The field is illustrative and reduced-order. It is not computational fluid dynamics and represents no particular city.

Table 3.3 Plant Parameters. Every Value Is Adjustable in the Model Dialog Over the Range Shown Unless Marked Hidden

Symbol	Meaning	Value	Range
m_e	empty mass	400 kg	300–500
I_e	empty pitch inertia	700 kg m^2	400–1200
ℓ	centroid to group thrust line	2.0 m	1.4–2.6
r_p	passenger radius of gyration	0.3 m	hidden
h_{cg}	skids to center of mass	1.1 m	hidden
h_r	rotor plane above center of mass	0.8 m	hidden
r_{rot}	rotor radius for strikes	0.75 m	hidden
—	skid half-length	1.2 m	hidden
T_{max}	group thrust rating	4200 N	3000–6000
T_{idle}	idle thrust per group	150 N	0–600
τ_T	group thrust lag	0.12 s	0.03–0.4
A	disk area per group	12 m^2	6–20
FM	overall figure of merit	0.6	0.4–0.8
C_dA_x, C_dA_z	drag areas	8, 24 m^2	2–16, 6–40
h_{cp}	pressure center above mass center	0.4 m	−0.5–1.2
ρ	air density	1.225 kg/m^3	1.0–1.3
g	gravity	9.81 m/s^2	hidden
E_{cap}	usable battery energy	24 kWh	12–40
P_{max}	rated battery power	190 kW	120–300
s_k, p_f	sag knee, power at empty	35, 50 %	10–60, 20–100
P_{av}	avionics and cabin power	1.5 kW	0–5
θ_{max}	tilt command limit	15°	5–30
—	sink that breaks the gear	2.5 m/s	1–5
—	tilt that tips over at touchdown	12°	4–25
σ_x, σ_v	position, velocity noise	0.05 m, 0.03 m/s	0–0.5, 0–0.3
σ_θ, $\sigma_{\dot\theta}$	tilt, gyro noise	0.1°, 0.3 °/s	0–1, 0–3
α	profile exponent	0.28	0.1–0.45
k_{gap}	gap speed-up	1.5	1–2
L_w, k_s	wake length, shelter depth	2.5H, 1.05	1–5, 0.5–1.2

3.3.5 Battery and Available Thrust

Hover momentum theory gives the induced power of an actuator disk as $T^{3/2}/\sqrt{2\rho A}$ [12], and an overall figure of merit FM folds in profile power, motors and inverters, as shown in Equation (3.6).

$$\begin{aligned} \dot{E} &= -\left[\sum_{i=L,R} \frac{T_i^{3/2}}{FM\sqrt{2\rho A}} + P_{av}\right] \\ T_{avail} &= \min\left(T_{max},\ \left[P_g\, FM\sqrt{2\rho A}\right]^{2/3}\right) \\ P_g &= \tfrac{1}{2}\left[P_{max} f(s) - P_{av}\right] \end{aligned} \tag{3.6}$$

where A is the disk area of one group, $s = E/E_{cap}$ the state of charge, and $f(s) = 1$ above the knee s_k and $p_f + (1-p_f)s/s_k$ below it, as the pack voltage sags. At 490 kg the vehicle draws 73.9 kW to hover. The battery limit binds below a charge of 27.2 %, at 17 % a group can deliver 3.72 kN instead of its 4.2 kN rating, and an empty battery delivers nothing. The lift-plus-cruise aircraft of Chapter 4 meets the same limit, a battery that bounds power as well as energy.

3.3.6 Contact, Strikes and Numerics

A touchdown occurs when the skids reach a surface moving down, either z at least 5 mm below the roof height with $\dot{z} < 0$ or a skid end at the surface sinking faster than 0.02 m/s, and the second test is ignored for 0.5 s after liftoff so that a skid rocking off the roof it just left is not a landing. A touchdown in the street, beyond 12° of tilt or faster than 2.5 m/s is a crash, one more than 3 m from a pad center is a building violation, and a rotor tip inside a building, or a skid end more than 0.15 m inside one, is a strike. Otherwise the vehicle is set level with zero velocity and the touchdown speed and pad error

are recorded. Liftoff requires $T\cos\theta > mg$ and is suppressed for 0.3 s after a touchdown, so that a vehicle that touched down carrying almost its weight does not bounce. The parameters are listed in Table 3.3. The states advance by classical fourth-order Runge-Kutta at 2 ms, control executes at 100 Hz, and the log is written at 20 Hz, on the engine of Section 1.6.1. Halving the step, with control still at 100 Hz, moves the touchdowns of the graded route by at most 0.04 mm/s and 0.02 mm with the suggested controller and 0.04 mm/s and 0.06 mm with the shipped one. A scenario starts either on a pad at idle thrust with the load still to board, or in the air trimmed for its load, with the battery at the charge the case sets.

3.3.7 Assumptions

Flight is planar. There is no yaw, roll or sideslip and no wind out of the plane, so the wind of the application is a crosswind to the vertical takeoff and landing paths, and a vehicle flying toward $-x$ flies backward rather than turning.

Each side is one rotor group with a first-order thrust lag. Rotor inflow dynamics, blade flapping and the rotor H-force are absent, and those effects change thrust and moment with airspeed and angle of attack [8]. A real rotor at fixed speed gains or loses thrust in a vertical gust far more strongly than the quadratic drag here, so vertical gusts are understated in calm air.

Drag uses fixed areas in the earth frame, which holds for the small tilts of low-speed flight. Wingborne cruise and rotor tilting are outside the model.

Power follows hover momentum theory with a constant figure of merit, without climb, descent or forward-flight corrections and without vortex-ring state [12]. The battery is an energy store with a sagging power limit and no voltage dynamics, temperature or aging.

The wind field is a set of closed-form patches tuned to the qualitative features of flow around buildings [6]. Turbulence is temporal colored noise scaled by a position-dependent intensity, the same at both groups, and wakes neither meander nor shed vortices.

The skids are rigid, touchdown is instantaneous and sets the vehicle level, and there is no ground effect. Navigation measurements carry small colored noise with no latency, bias or satellite dropouts, which between real buildings are a problem of their own. The rotor radius used for strikes, 0.75 m, is smaller than the 0.98 m implied by the disk area of four 1.95 m rotors per group, so clearance is slightly optimistic.

3.4 Three Loops and Three Levels of Knowledge

The flight controller runs every $\Delta t_c = 10$ ms on sampled navigation measurements and never reads the true state, mass, center of mass or wind. Position and height carry colored noise of standard deviation σ_x with a 0.5 s correlation time, the velocities σ_v with 0.05 s, the tilt σ_θ with 0.05 s and the rate gyro $\sigma_{\dot\theta}$ with 0.02 s. The loop structure is shown in Figure 3.3.

3.4.1 The Shared Loop Algorithm

All three loops use the framework's velocity-form PID of Section 1.6.2, written in this chapter's symbols in Equation (3.7).

$$
\begin{aligned}
e_k &= a\,(\mathrm{SP}_k - \mathrm{PV}_k), \qquad P_k = K_c e_k \\
S_k &= S_{k-1} + (P_k - P_{k-1}), \qquad c_k = b_k + S_k + I_{k-1} \\
u_k &= \mathrm{clamp}(c_k,\ u_{min,k},\ u_{max,k}) \\
I_k &= I_{k-1} + \left[\frac{K_c}{\tau_I} e_k + \frac{u_k - c_k}{T_t}\right] \Delta t_c
\end{aligned}
\tag{3.7}
$$

where $a = \pm 1$ is the action and b_k is a bias recomputed every step. In the symbols of Equations (1.19) to (1.22), c_k is the output before limiting v_k and b_k takes the place of u_b. The running sum S_k telescopes to $K_c e_k$ for whatever gain is in force, which keeps a scheduled gain meaning the gain, and

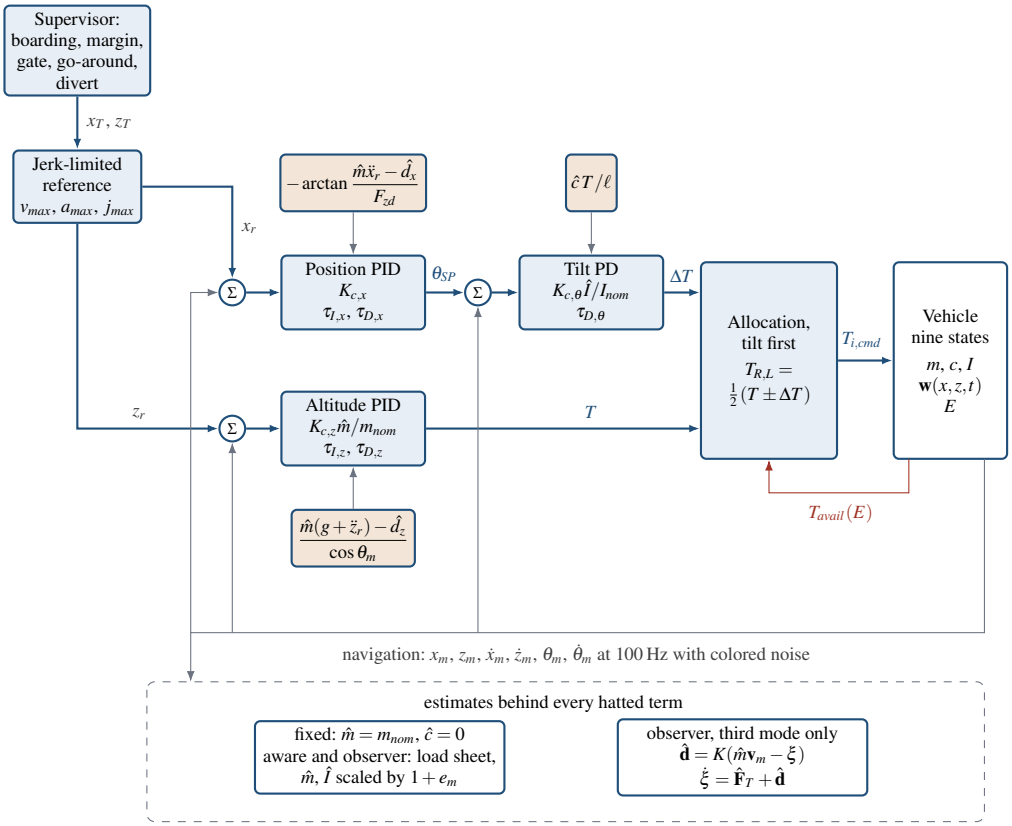


Figure 3.3 Three loops, what they are told and what supervises them. The position loop owns no actuator and writes the tilt setpoint θ_{SP}, the tilt loop writes the differential thrust ΔT, and the altitude loop writes the total thrust T. The shaded blocks are feedforward terms built from the estimates, which are the design point in fixed tuning, the load sheet in the payload-aware mode, and the load sheet with the observer's force estimate $\hat{\mathbf{d}}$ in the third mode. The allocation serves the tilt first within the available thrust, and the supervisor sets the targets of the reference generator.

back-calculation uses $T_t = \tau_I$. No output is rate limited, so the group thrust lag is the only actuator dynamics. The framework's own derivative on the measurement is set to zero in all three loops, and each derivative term is formed from measured rates and carried in b_k instead, so it produces no kick on a setpoint change. Each loop has its own manual and automatic switch, and transfer in either direction is bumpless.

3.4.2 Altitude and Position

The altitude loop has $a = +1$ and is reverse acting in the convention of Section 1.3, because more thrust raises the vehicle, and its bias is the weight feedforward plus the derivative term, as shown in Equation (3.8).

$$
\begin{aligned}
b_z &= \frac{\hat{m}(g + \ddot{z}_r) - \hat{d}_z}{\max(\cos\theta_m,\, 0.5)} + K^e_{c,z}\tau_{D,z}\,(\dot{z}_r - \dot{z}_m) \\
T &\in \left[2T'_i + |\Delta T|,\; 2T_{avail} - |\Delta T|\right]
\end{aligned}
\tag{3.8}
$$

with $T'_i = \min(T_{idle}, T_{avail})$ and the upper bound never below the lower, where $\hat{m}$ is the mass the controller believes, $\hat{d}_z$ the observer's vertical force estimate (zero unless the third mode is selected),

z_r the reference and $K^e_{c,z}$ the gain in force. On the pad the bias sits at idle, and the 1.5 s spool-up ramps it from idle to the hover feedforward.

The position loop has $a = -1$ and is direct acting, because a positive tilt accelerates the vehicle toward $-x$, and its output is the tilt setpoint, limited to $\pm\theta_{max}$, with a feedforward for the reference acceleration and the estimated force, as shown in Equation (3.9).

$$\begin{aligned} b_x &= -\arctan\frac{\hat{m}\ddot{x}_r - \hat{d}_x}{F_{zd}} - K_{c,x}\tau_{D,x}\left(\dot{x}_r - \dot{x}_m\right) \\ F_{zd} &= \max\left(0.2\hat{m}g,\ \hat{m}(g+\ddot{z}_r) - \hat{d}_z\right) \end{aligned} \tag{3.9}$$

Both derivative terms act on measured velocity against the reference's own velocity, so the reference supplies its own rate feedforward.

3.4.3 Tilt Loop and Allocation

The tilt loop is proportional-derivative and reverse acting, because more differential thrust raises the tilt, with the rate term on the gyro and the trim of Equation (3.2) fed forward, as shown in Equation (3.10).

$$\Delta T = K^e_{c,\theta}\left[(\theta_{SP} - \theta_m) - \tau_{D,\theta}\dot{\theta}_m\right] + \frac{\hat{c}\,T_{k-1}}{\ell} + I_{k-1} \tag{3.10}$$

with $|\Delta T| \le T_{avail} - T_i'$. It has no reset action, so the term I holds only the value left by a manual transfer or by the trim of an airborne start, and it is multiplied by $\mathrm{e}^{-\Delta t_c/1.5\,\mathrm{s}}$ every step so that the transfer bias bleeds away in automatic. The allocation gives $T_{R,L} = (T \pm \Delta T)/2$. Because the total thrust is limited to what the differential leaves, each group stays between idle and the available thrust, and a group at its limit costs altitude, never attitude. Section 1.4.7 sets this priority beside other allocation rules.

3.4.4 What Each Mode Knows

Fixed tuning believes the design point, $\hat{m} = m_{nom} = 480\,\mathrm{kg}$, $\hat{c} = 0$ and $\hat{I} = I_{nom} = I_e + (m_{nom} - m_e)r_p^2 = 707.2\,\mathrm{kg\,m^2}$, and keeps its gains. The payload-aware mode reads the load sheet written when boarding closes and computes $\hat{m}$, $\hat{c}$ and $\hat{I}$ from Equation (3.3), with $\hat{m}$ and $\hat{I}$ multiplied by $1 + e_m$ to represent an error in the declared weights. It schedules the gains as $K^e_{c,z} = K_{c,z}\hat{m}/m_{nom}$ and $K^e_{c,\theta} = K_{c,\theta}\hat{I}/I_{nom}$. The third mode adds the observer's estimates $\hat{d}_x$ and $\hat{d}_z$ to the two feedforward terms. The observer runs in every mode, so its estimate can be watched, but only the third mode uses it.

3.4.5 The Disturbance Observer

Each translational axis has a generalized-momentum observer, the observer of Section 1.4.3 applied to the two axes, as shown in Equation (3.11).

$$\begin{aligned} \xi_{k+1} &= \xi_k + \left(\hat{F}_{T,k} + \hat{d}_k\right)\Delta t_c \\ \hat{d}_{k+1} &= K\left(\hat{m}v_{m,k} - \xi_{k+1}\right) \\ \hat{\mathbf{F}}_T &= \hat{T}\left(-\sin\theta_m,\ \cos\theta_m\right) - \hat{m}g\,\mathbf{e}_z \end{aligned} \tag{3.11}$$

where $\hat{T}$ is the sum of the controller's own group commands passed through an exact discrete model of the 0.12 s lag, and $K = 1.5\,\mathrm{rad/s}$ is the bandwidth. For the linear model with the thrust known exactly, $\hat{d} = Kd/(s+K)$, so a step force is estimated with a time constant of $1/K = 0.67\,\mathrm{s}$. The observer sees drag, pushes and any weight the load sheet missed as one force, because a mass error $\Delta m = m - \hat{m}$ appears as $-\Delta m(g + \ddot{z})$. On the ground it is reset to zero. The vessel observer of Chapter 6 carries wind and current the same way, as a slowly varying force that it feeds forward.

Table 3.4 Controller, Reference and Supervisor Settings as Shipped

Symbol	Meaning	Value
$K_{c,z}$, $\tau_{I,z}$, $\tau_{D,z}$	altitude PID at m_{nom}	700 N/m, 6, 1.6 s
$K_{c,x}$, $\tau_{I,x}$, $\tau_{D,x}$	position PID	3.5 °/m, 12, 2.0 s
$K_{c,\theta}$, $\tau_{D,\theta}$	tilt PD at I_{nom}	120 N/°, 0.35 s
m_{nom}	design mass of the fixed tuning	480 kg
K	observer bandwidth	1.5 rad/s
v_{max}	horizontal speed limit	10 m/s
a_{max}, j_{max}	acceleration and jerk limits	1.2 m/s^2, 1.0 m/s^3
—	climb, descent, final, flare speeds	3, 2.5, 1.2, 0.35 m/s
μ_{min}	dispatch thrust margin	25 %
—	cruise band	10 m over roofs, ±6 m
—	shaft over each pad	±8 m
—	gate height and window	8 m, 1.0 m, 0.5 m/s
—	gate dwell and longest wait	1, 6 s
—	final go-around, flare height	1.5 m, 3 m
—	go-around wait, divert	3 s, at the third
—	saturation divert	2.5 s, climb or cruise

HISTORY Estimating the Load Torque (Early 1980s)

The disturbance observer was put forward in motion control in the early 1980s, to improve the torque and speed control of a motor by estimating its load torque. Related estimators followed, among them the extended state observer of the 1990s, the core of active disturbance rejection control. All of them lump the external disturbance and the uncertainty of the model together and estimate the total from measured variables, so that the controller can cancel it. Over four decades the idea has reached robot manipulators, motion servos, magnetic levitation, power converters and disk drives. In aeronautics and astronautics its purpose is to cope with disturbance forces and torques caused by external winds, unmodeled dynamics or uncertain aerodynamics [2]. The third controller mode of this chapter applies the idea to the force on each translational axis.

3.4.6 Reference and Supervisor

Each axis follows an online jerk-limited reference, which moves toward its target with the acceleration changing no faster than j_{max} and capped at a_{max} and the speed at the phase limit, and begins braking the moment the distance left equals the exact jerk-limited stopping distance, checking the next substep so that it brakes early rather than overrun that point. It re-plans from its present state whenever the target moves, first stopping any motion away from a new target, which is what a go-around or a changed setpoint needs, and online generation of this kind is established in robotics [19]. Section 1.4.4 gives the durations and peaks of jerk-limited profiles. While it turns back toward a target it builds only the acceleration that the stop to follow leaves room for, and a stop that comes too late, from a moving start, re-plans from where it crosses the target instead of hunting about it. A sweep of 78 000 moves over the slider ranges, from rest and from moving starts, settles every one. It takes ten substeps per control step, and a linear third-order capture filter removes the last few centimeters.

The supervisor boards the load at each stop and then applies the dispatch rule, departing only if the thrust margin $\mu = 2T_{avail}/(\hat{m}g) - 1$ is at least $\mu_{min} = 25\,\%$ and holding on the pad otherwise. After a 1.5 s spool-up it climbs to the leg's cruise band, cruises and descends to an approach gate 8 m above the pad. It continues below the gate only once the vehicle has been within 1.0 m of the pad center and slower than 0.5 m/s sideways for 1 s, and it waits up to 6 s for that. The final descent aims 1 m into the roof at 1.2 m/s, slowing to 0.35 m/s below 3 m, and goes around if the vehicle drifts 1.5 m off center. A go-around climbs back to the band, waits 3 s and approaches again, and the third go-around at one pad diverts the vehicle back to its departure pad. A diverted approach that fails the same way ends in an emergency landing at that pad without the gate test, and the route is marked aborted. Thrust at the available limit for 2.5 s in the climb or the cruise also diverts. In the air the margin is recomputed from $\hat{m}g - \hat{d}_z$ filtered with 1.5 s, for display only. Table 3.4 gathers every setting.

Three models are distinguished throughout. What is simulated is Equations (3.1) to (3.6) together with the wind of Table 3.2. The controller's internal model is algebraic, the believed mass, center of mass and inertia, the hover force balance of the two feedforward terms, and the observer's translational momentum balance with the rotor lag. The analysis model of Section 3.5 is the linearization about level hover, used to interpret the results and present nowhere in the code.

3.5 What a Loop Must Be Told

3.5.1 Linearized Loops and Their Separation

About level hover with $c = 0$ and $T = mg$, Equation (3.2), the thrust lag and the tilt law give the closed tilt loop of Equation (3.12).

$$\frac{\theta}{\theta_{SP}} = \frac{\kappa}{\tau_T I s^3 + I s^2 + \kappa \tau_{D,\theta} s + \kappa}, \qquad \kappa = \ell K_{c,\theta} \tag{3.12}$$

With $I_{nom} = 707.2\,\mathrm{kg\,m^2}$ and $\kappa = 13.75\,\mathrm{kN\,m/rad}$, and without the thrust lag, the loop would have a natural frequency of 4.41 rad/s and a damping ratio of 0.77. The 0.12 s lag turns this into a pair at 6.27 rad/s damped at only 0.34, plus a real root at $4.12\,\mathrm{s^{-1}}$. The linear model predicts 0.417 s to 63 % of a step with 9.4 % overshoot, and the full simulation with the navigation noise switched off gives 0.413 s and 10.1 % for a 5° step in the tilt command, timed from the controller execution that applies it.

For the position loop with an ideal inner loop, $\ddot{x} = -g\theta$ and the PID of Equation (3.9) give the characteristic equation $s^3 + gK_{c,x}\tau_{D,x}s^2 + gK_{c,x}s + gK_{c,x}/\tau_{I,x} = 0$, a pair at 0.70 rad/s with a damping ratio of 0.79 and a real root at $0.10\,\mathrm{s^{-1}}$. Closing both loops with Equation (3.12) inside puts the tilt pair at 5.84 rad/s with a damping ratio of 0.37, the position pair at 1.07 rad/s with a damping ratio of 0.88, and real roots at 2.01 and $0.103\,\mathrm{s^{-1}}$, a separation of 5.5 between the two oscillatory modes, the separation a cascade needs by Section 1.4.3. The rocket of Volume 3, Chapter 10 has the same structure, a position loop that owns no actuator and commands an attitude.

With a correct feedforward the altitude error obeys $m\ddot{e} = -K^e_{c,z}[e + \tau_{D,z}\dot{e} + \int e\,dt/\tau_{I,z}]$ through the thrust lag. Scheduling $K^e_{c,z} \propto \hat{m}$ keeps the roots at 0.27, 0.58, 2.71 and $4.78\,\mathrm{s^{-1}}$ for every load. Fixed gains at 620 kg give a pair at 0.99 rad/s with a damping ratio of 0.98 and real roots at 0.26 and $6.12\,\mathrm{s^{-1}}$, still well damped, so the heavy leg is not a gain problem. Setting the fixed tuning's design mass to 620 kg, which corrects its feedforward and leaves its gain at 700 N/m, holds the heavy climb of case 3 within 0.05 m, and the payload-aware mode with its gain held at the same effective 700 N/m ($K_{c,z} = 540\,\mathrm{N/m}$, scheduled to 698 N/m at 620 kg) gives 0.05 m as well, against 1.78 m for the shipped fixed tuning. The feedforward does the work.

🕮 **Pause.** Try Exercise 3.3 before reading on.

3.5.2 The Error Budget

A loop that is not told about a force F can oppose it only through its error, as Equation (1.4) states for the cart of Chapter 1. The proportional term alone would need $e_P = F/K_P$, where K_P is the force per unit error, and the integral then removes that error over a time of order τ_I. For the altitude loop $e_P = \Delta mg/K^e_{c,z}$, for the position loop $e_P = \arctan(F/mg)/K_{c,x}$, and for the tilt loop, which has no integral, the error is permanent at $e_P = mgc/(\ell K^e_{c,\theta})$. The predictions and the measured errors are compared in Table 3.5.

🕮 **Pause.** Try Exercise 3.1 before reading on.

The tilt loop matches its budget to 0.01°, because nothing else can supply the moment. The loops with integral action reach 90 to 102 % of their proportional-only error, because the integral is slow against the rise of the force. The one exception, the C to D climb of the graded route at 108 %, climbs out of the jet over pad C. The vertical drag of Equation (3.4) grows with the whole airspeed, so climbing through an 11 m/s crossflow adds a downward force of about 350 N that the budget

Table 3.5 Error a Loop Needs to Supply a Force It Was Not Told About. e_P Is the Proportional-Only Value and the Last Column the Measured Peak or Standing Error

Case, mode	Unknown force	e_P	Measured
3, fixed, heavy climb	$\Delta mg = 1.37\,\text{kN}$	1.96 m	1.78 m
4, aware, $e_m = -20\,\%$	1.22 kN	1.68 m	1.54 m
11, fixed, B → C climb	1.18 kN	1.68 m	1.51 m
11, fixed, C → D climb	1.37 kN	1.96 m	2.11 m
6, aware, crosswind	345 N, 4.1°	1.17 m	1.19 m
5, fixed, steady hover	$mgc/\ell = 294\,\text{N}$	2.45°	2.46°

Table 3.6 Scenarios. Wind Is the Background Speed U_0 at 50 m

#	Set-up	Lesson
1	hover 10 m over A, push at 8 s	thrust equals weight, tilt to move
2	A → B, a_{max} 2.5, j_{max} 4, v_{max} 12	comfort, time and energy
3	A → B → C, fixed, heavy second leg	feedforward from a known load
4	B → C, load sheet 20 % light	an estimate repairs the sheet
5	A → B, 40 kg bag at $x_b = -1.5$	trim for the center of mass
6	hover over the street, wind 0 to 8	a steady force and its estimate
7	B → C, wind 9	hovering in the gap's jet
8	C → D, wind 11, turbulence 1.3	an integral that remembers
9	B → C, full load, 17 % charge	dispatch margin
10	B → C, wind 6, gust front at the gate	stabilized approach, go-around
11	B → C → D, wind 11, 36 % charge	graded route

leaves out, and even the payload-aware mode, whose weight is right, lags 0.37 m on that climb. An estimate removes the error on the observer's time scale instead, and the push test in hover confirms the first-order behavior. With the navigation noise switched off, the estimate of a 600 N push reaches 63 % after 0.66 s at $K = 1.5\,\text{rad/s}$, 2.00 s at 0.5 and 0.33 s at 3 rad/s, each within one 10 ms controller period of $1/K$.

A proportional-integral loop that begins and ends with no standing force must also integrate zero error, so an excursion in one direction has to be repaid in the other. After the 600 N push of case 1 with the noise switched off, the vehicle overshoots its setpoint by 0.31 m and the two lobes of the error have equal areas, 3.72 m s each over the 142 s after the push.

3.6 Scenarios and Measured Results

The ten cases and the graded route are listed in Table 3.6. Every value below was measured on the engine at the default seed with the case as shipped unless a change is named, a named change being made before the run starts (Section 1.6.4), and the principal results are collected in Table 3.7.

3.6.1 Hover and Tilt

Before the push at 8 s, case 1 carries 490 kg on 4.80 kN, the weight to within 0.04 %, holds within 0.07 m sideways, and draws 73.9 kW. The 600 N push moves the vehicle 1.46 m, tilting it up to 9.4° on the way back, and it passes back through the setpoint 5.20 s after the push began. It then overshoots by 0.30 m and is not back within 0.1 m until 28.3 s, which is the repayment of Section 3.5 with noise added. With the position loop in manual at −5° from 15 to 22 s, the vehicle accelerates toward $+x$ at $0.66\,\text{m/s}^2$ between four and seven seconds in, below $g\tan 5^\circ = 0.86\,\text{m/s}^2$ because the drag grows with speed, and it covers 18.1 m and reaches 5.0 m/s. Back in automatic, it is within 0.5 m of the setpoint again 18.4 s later.

Table 3.7 Measured Results. Aware Is the Payload-Aware Mode and Observer the Mode With the Wind Estimate

#	Condition	Result
1	before the push	$T/mg - 1 = -0.04\,\%$, 73.9 kW, $\lvert\Delta x\rvert \leq 0.07$ m
1	600 N, 2 s push	peak 1.46 m, back through at 5.20 s, overshoot 0.30 m, tilt $\leq 9.4°$
1	manual $-5°$, 7 s	0.66 m/s^2, 18.1 m, 5.0 m/s
2	as shipped	2.84, 5.36 m/s^3, 6.95 s at limit, lag 5.7 m, 35.3 s, 0.76 kWh
2	a_{max} 1.2, j_{max} 1.0	1.59, 1.75 m/s^3, no saturation, lag 0.66 m, 43.2 s, 0.92 kWh
3	fixed	climbs 0.09 m and 1.78 m behind, heavy liftoff 1.03 s later than aware
3	aware	heavy climb 0.05 m
4	aware	liftoff 1.17 s after climb start, lag 1.54 m, 0.88 m at 5 s
4	observer	lag 0.83 and 0.02 m at 1 and 3 s, then 0.44 m above, $\hat{d}_z = -1.21$ kN
5	fixed	3.15°, 0.76 m in 4 s, 2.27° at gate
5	aware	0.30°, 0.07 m, 0.08° at gate
6	aware, observer	drift 1.19, 0.36 m, back in 19.6, 8.3 s
7	aware, observer	wander 1.90, 0.41 m, gate 1.39, 0.24 m, land 0.71, 0.18 m
8	aware, observer	worst 0.98, 0.33 m, land 0.19, 0.07 m
9	full load	3.72 kN per group, $\mu = 22.4\,\%$, holds
9	one passenger off	$\mu = 45.9\,\%$, departs 3.4 s later
10	aware	go-around 43.2 s, lands 73.9 s at 0.62 m, 1.41 kWh
10	observer	go-around 45.0 s, lands 76.6 s at 0.02 m

3.6.2 Comfort and the Reference

Case 2 lets the reference accelerate at 2.5 m/s^2, which is 95 % of the $g\tan 15° = 2.63\,\mathrm{m/s^2}$ that the tilt limit allows, so the corrections the loop adds push it onto the limit. The tilt command sits there for 6.95 s, the vehicle trails its reference by up to 5.7 m, and the comfort signals peak at 2.84 m/s^2 and 5.36 m/s^3 on the kinematic acceleration filtered at 0.2 s, while liftoff to touchdown takes 35.3 s. At 1.2 m/s^2 and 1.0 m/s^3 the hop takes 43.2 s, peaks at 1.59 m/s^2 and 1.75 m/s^3, never saturates, trails by 0.66 m and lands 0.10 m from the center instead of 0.25 m. Because hover power is paid by the second, the gentle hop uses 0.92 kWh against 0.76 kWh.

3.6.3 The Load and the Load Sheet

Case 3 flies fixed tuning designed for 480 kg, first with one 80 kg passenger and then with two 100 kg passengers and 20 kg of bags. Measured over the last half second of each gate dwell, the hover thrust rises from 4.65 to 6.03 kN, a ratio of 1.298 against a mass ratio of 1.292. The light climb stays within 0.09 m of its reference and the heavy one falls 1.78 m behind, because 1.37 kN of weight has to come from the error, and the heavy liftoff comes 1.03 s later than with the payload-aware mode, whose heavy climb stays within 0.05 m. The climber of Volume 3, Chapter 12 carries a gravity feedforward for the same reason, because its effective weight changes along its route. The error of a wrong feedforward has either sign. With the design mass set to 620 kg, the light climb rises 1.74 m above its reference and lifts off 0.22 s before the climb begins, during the spool-up.

Case 4 gives the payload-aware mode a load sheet 20 % light, 124 kg on a 620 kg vehicle and 1.22 kN of weight it does not know. The spool-up stops short of the weight, so the vehicle sits on the pad until the altitude error has built enough thrust, and it lifts off 1.17 s after the climb begins instead of 0.23 s, falls 1.54 m behind, and is still 0.88 m behind five seconds after liftoff. The observer cannot see a weight the pad carries, so its liftoff is just as late. Once airborne it sees the missing weight as a downward force, and the lag is 0.83 m one second after liftoff and 0.02 m after three. The estimate then arrives on top of a proportional term still correcting the lag, and the vehicle overshoots to 0.44 m above its reference 4.5 s after liftoff. Over the last two seconds before touchdown the estimate averages −1.21 kN of the 1.22 kN missing.

🕮 **Pause.** Try Exercise 3.2 before reading on.

3.6.4 Balance

Case 5 puts a 40 kg suitcase at the left end of the tray. Fixed tuning, which does not know, tilts 3.15° and wanders 0.76 m in the four seconds after liftoff and flies the approach gate with 2.27° between the tilt it is asked for and the tilt it has, while its differential thrust averages −286 N against the −294 N trim. In the steady hover of case 1 with the same load, chosen before Run so that the airborne start carries it, the standing error averages 2.46° from 20 to 40 s, the budget of Table 3.5. The payload-aware mode feeds the trim forward and holds 0.30° and 0.07 m after liftoff and 0.08° at the gate, and in a steady hover its differential thrust matches mgc/ℓ to within 0.1 %.

3.6.5 Steady Wind, the Gap and the Wake

Case 6 steps the background wind from calm to 8 m/s while the vehicle hovers 60 m over the street, where the wind averages 8.36 m/s from 50 to 90 s and the drag settles at 345 N with the vehicle leaning 4.1°. Without an estimate it drifts 1.19 m, 7.2 s after the step, and needs 19.6 s to pass back within 0.1 m, because only the integral can build the standing tilt. With the observer, whose steady estimate is within 1.3 % of the drag, it drifts 0.36 m and is back in 8.3 s.

> **TRY IT IN THE APP 6 · Steady Crosswind**
>
> Load the case and press Run. Watch the Horizontal air force trend: as the wind steps from calm to 8 m/s, the drag settles near 345 N and the dashed estimate follows it. Then watch the Horizontal position trend. With the payload-aware controller the vehicle drifts 1.19 m downwind and needs 19.6 s to pass back within 0.1 m.

The observer bandwidth is a trade. Across K from 0.3 to 4 rad/s in case 6, the peak drift falls from 0.67 to 0.24 m, while the standard deviation of the tilt command in the steady wind rises from 1.08 to 1.35°, against 1.01° without an estimate, both over 50 to 90 s. The estimate error is smallest, 34 to 35 N standard deviation, at 1.0 to 1.5 rad/s, because slower estimates lag the turbulent drag and faster ones pass the velocity noise through the gain $K\hat{m}$, and the shipped 1.5 rad/s sits on that flat minimum.

Case 7 flies B to C in a 9 m/s wind. Cruising through the gap the vehicle moves with the 12.9 m/s channeled flow and averages only 4.5 m/s of airspeed and 112 N of drag, but over pad C, where the jet leaves the gap, it must hover in about 11 m/s against a drag that averages 571 N over the gate dwell. Without an estimate the position loop needs an error and then its integral, and the vehicle wanders up to 1.90 m off the pad line on the way down, 1.39 m at the gate, and lands 0.71 m from the center, outside the 0.5 m target. With the observer it is 0.24 m at the gate and lands 0.18 m from the center. The landing depends on the seed. Over seeds 1 to 10 the payload-aware mode lands 0.21 to 0.91 m from the center, outside the target five times, and wanders 1.12 to 2.04 m, while the observer lands within 0.27 m every time and wanders 0.27 to 0.83 m.

Case 8 crosses the 58 m tower in an 11 m/s wind with the turbulence scaled by 1.3 and descends to the clinic in its wake. At the top of the descent, 68 m up in the tower's shear layer, the mean wind of the field is 5.7 m/s with turbulence of 4.4 m/s standard deviation, and the payload-aware mode's position integral holds 3.3° of lean. By 55 m the mean wind has fallen to 2.1 m/s, yet the integral still holds 3.3° there and 1.5° at the gate, so the vehicle leans on air that is no longer there. It is 0.98 m off the pad line at the top and up to 0.73 m below 60 m, and lands 0.19 m from the center. The observer drops its feedforward as the force goes, keeps the error to 0.33 m and lands 0.07 m from the center. Knowing the force also means asking for all of it, and while braking over the clinic the observer mode holds the tilt command at 15° for 1.55 s, which the payload-aware mode never does. The peak jerks of the two runs, 8.4 and 9.2 m/s^3, both come at the cruise band over the clinic, where the vehicle flies through the tower's shear layer.

3.6.6 Battery and the Approach

Case 9 boards a full load, two 100 kg passengers and 20 kg of bags, on a battery at 17 %. The power limit has sagged to 74 % of its rating, a group can deliver 3.72 kN, and against the 6.08 kN weight

Table 3.8 Graded Route at the Default Seed

	Fixed	Aware	Observer
climb lag B → C, C → D (m)	1.51, 2.11	0.10, 0.37	0.07, 0.15
pad C error (m), sink (m/s)	0.99, 0.45	0.98, 0.45	0.23, 0.41
pad D error (m), sink (m/s)	0.05, 0.33	0.05, 0.34	0.00, 0.38
tilt limit (s)	2.2	2.8	2.9
battery left (%)	22.5	22.4	22.6
route complete (s)	133.9	134.0	132.9
verdict	fail	fail	pass

the margin is 22.4 % when the hold begins, below the 25 % rule, so the supervisor holds on the pad. Taking one passenger off raises the dispatch margin to 45.9 %, and the vehicle departs 3.4 s after the change, the time for the passenger to walk off and the check to pass. What the supervisor knows matters as much as what the loops know. The fixed mode judges the margin on its 480 kg design mass, reads 58 %, and takes off with the full load, and because the true margin of 22 % still covers the flight it lands on C 0.07 m from the center without saturating, while the in-flight margin reads 23 % once the observer has seen the weight and falls to 14 % on the final approach as the battery drains. The rule protects a reserve, not a hard limit.

Case 10 flies B to C in a 6 m/s wind and times a gust front of 8 m/s over 12 s to the vehicle's arrival at the gate, at 38.8 s. The vehicle clears the gate check before the gust has built, starts down at 39.8 s, and is pushed 1.5 m off center at 43.2 s, a go-around. With the gust at its peak the tilt command sits on its limit for 3.0 s while the vehicle climbs back. It starts the second approach at 55.0 s with the gust gone and lands at 73.9 s, 0.62 m from the center, in the jet of case 7 again. The leg costs 1.41 kWh, against 0.94 kWh in a model run with the gust removed, which the case itself does not offer. With the observer the go-around comes at 45.0 s and the second approach lands 0.02 m from the center at 76.6 s. Three 600 N pushes in a row at the start of every final approach show the divert rule. The vehicle goes around at 41.4, 71.8 and 94.2 s, diverts to B at 105.7 s, goes around three more times there and makes an emergency landing on B at 195.2 s, which marks the route aborted.

3.6.7 The Graded Route

The graded route flies hotel, offices and clinic in an 11 m/s wind, boarding two 90 kg passengers and 20 kg of bags at B, a tray position of −1.2 m, and a swap to two 100 kg passengers at C, on a battery that starts at 36 %. It is met with no crash, off-pad touchdown or corridor excursion, every touchdown within 0.5 m of the pad center at under 0.5 m/s, and at least 20 % battery at the end. The three modes are compared in Table 3.8, and Figure 3.5 draws its distances as bars.

Shipped with fixed tuning, the route completes with no violation and 22.5 % left, but the heavy climbs fall 1.51 and 2.11 m behind and the vehicle lands 0.99 m from the center of pad C in the gap's jet, so the scorecard reads one touchdown of two in specification. The payload-aware mode repairs the climbs, to 0.10 and 0.37 m, but not the jet, landing 0.98 m off, and its worst altitude error on the first leg, 0.45 m, comes in the descent into the jet rather than in the climb. The observer repairs both, seeing the load the fixed tuning does not know as a vertical force and the jet as a horizontal one. It lands 0.23 m from the center of C and within 0.01 m of D's, at 0.41 and 0.38 m/s, the route is complete at 132.9 s, and the run ends 1.5 s later at 134.4 s with 22.6 % left. The pass leaves 0.27 m of the touchdown target, 0.09 m/s of the sink limit and 2.6 percentage points of battery to spare. Revealing the suggested setting and then pressing Reset gives the same run. The route is judged on the case as given, so a changed model parameter or disturbance setting voids the attempt. All three spend 2 to 3 s at the tilt limit descending into the jet, which the shaded band marks for the observer run in Figure 3.4.

The verdicts hold beyond the default seed. Over seeds 1 to 20 the observer passes all 20, with its worst touchdown 0.37 m from a pad center and its worst sink 0.491 m/s, while the fixed and

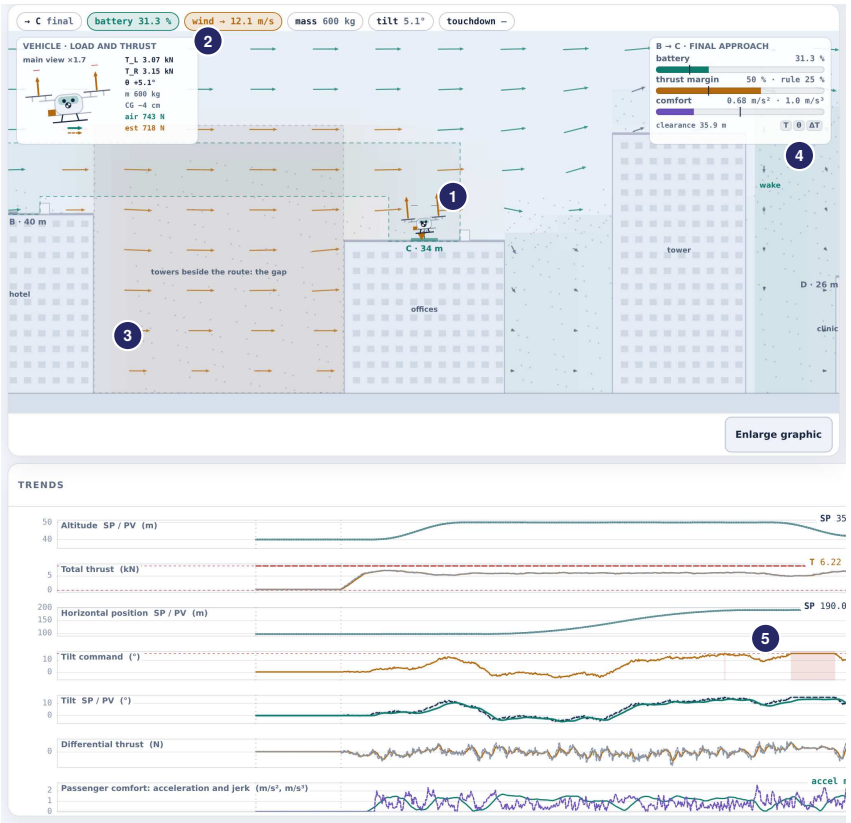


Figure 3.4 The graded route, Challenge · the afternoon route, with the suggested controller that adds the wind estimate, paused at $t = 47.00$ s on the final approach to pad C, cropped to the plant view and the trends. The vehicle (1), drawn 1.7 times its size, carries 600 kg with its center of mass 4 cm left of the centroid, hovers 1.9 m above the offices roof and leans 5.1° into a 12.1 m/s wind, the jet that the amber arrows trace through the gap between the towers beside the route (3). The dashed outline is the corridor of the leg from B, the triangle on the roof predicts a touchdown 0.6 m upwind of the pad center, the two ticks above it mark the approach gate, and the shaded, stippled zone labeled wake behind the tower holds weak, sinking flow over pad D (4). The close-up plate (2) compares the true horizontal air force of 743 N with the observer's 718 N, and the mission plate shows 31.3 % battery and a 50 % thrust margin against the 25 % rule. The trends hold 47 of the 60 s window, from boarding and spool-up on pad B through the climb to the 50 m cruise band, the move from 96 to 190 m and the descent, with the tilt command shaded where it sat at the 15° limit from 34.9 to 37.8 s (5), the tilt following its command, and the differential thrust and comfort signals below. The crop ends the trends a few seconds before the pause and cuts their readouts.

payload-aware modes pass 5 each, and every one of their 30 failures occurs at pad C. The margin on the touchdown speed is thin, and the observer's worst sink leaves 0.009 m/s to spare.

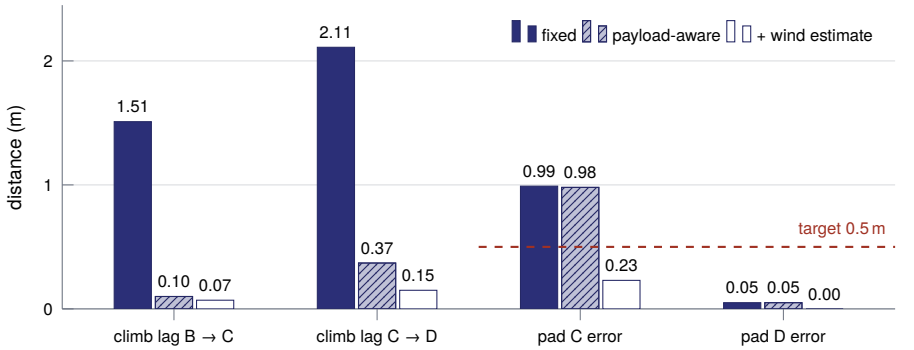


Figure 3.5 The graded route of Table 3.8 at the default seed, drawn as bars: the lag on the two heavy climbs and the touchdown error at pads C and D for the three controller modes. Notice that the load sheet of the payload-aware mode removes most of the climb lag but none of the miss at pad C, which sits in the gap's jet. Only the wind estimate brings that touchdown inside the 0.5 m target, and only it passes the route.

> ✦ DID YOU KNOW? **Knowing the Load Does Not Land in the Jet**
>
> From the simulator: on the graded route the payload-aware mode cuts the heavy climb lags from 1.51 and 2.11 m to 0.10 and 0.37 m, yet it lands 0.98 m from the center of pad C, no closer than fixed tuning at 0.99 m. Only the mode with the wind estimate lands within the target, at 0.23 m (Table 3.8).

3.7 Technology in Practice

The vehicle of Section 3.3 is read by one navigation system and moved by two rotor groups. A real multirotor fuses inertial and satellite measurements, drives its rotors with electric motors and flies under rules for its weight and balance. Figure 3.6 draws the chapter's three loops with such devices in place.

What Measures It

The navigation system NAV of Figure 3.1 stands for an inertial measurement unit, a satellite receiver and a filter that fuses them, as Section 1.4.6 describes. On a research quadrotor of 2007 an extended Kalman filter combined the satellite and inertial measurements into the full state [8]. In this chapter every measured state carries colored noise with no latency, bias or dropout, 0.05 m on position and 0.1° on tilt.

> TECHNOLOGY **Sensor: Inertial and Satellite Navigation**
>
> A multirotor takes its tilt and rates from an inertial measurement unit of three gyroscopes, three accelerometers and three magnetometers. On a research quadrotor of 2007 the attitude estimate was accurate to 2° as long as no acceleration was sustained, a sonic ranger gave the height above ground to 3 to 5 cm, and carrier-phase differential satellite navigation gave the position to 1 to 2 cm [8]. Between buildings the satellites are blocked or reach the receiver only by reflection. Such signals carry range errors of tens or even hundreds of meters, and the reported position can be wrong by the width of the street canyon [20]. The colored noise of a few centimeters in this chapter stands for none of this.

What Moves It

Each rotor group of the model lumps the four rotors on one side into one thrust, which follows its command through a lag of 0.12 s and never exceeds what the battery allows. On a small multirotor that thrust comes from brushless motors whose torque turns the rotors, and the voltage and current of each motor set its speed [8]. The simulator model of a six-passenger concept added each motor's

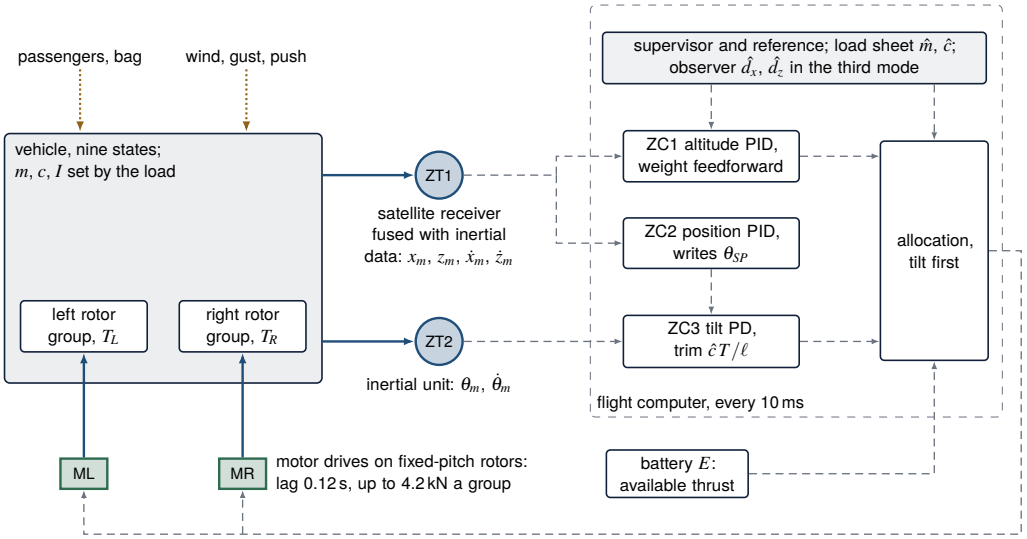


Figure 3.6 The three loops of the chapter with real devices in place of the schematic's symbols. ZT1 reads position and height from a satellite receiver fused with inertial data, ZT2 the tilt and its rate from the inertial unit, and one flight computer (dashed frame) runs the altitude, position and tilt loops (ZC1 to ZC3) every 10 ms. ML and MR are the motor drives of the two rotor groups, held within the thrust the battery allows. Notice that the position loop owns no motor: it writes the tilt setpoint, and only the allocation reaches ML and MR.

armature circuit and the inertia of its shaft and rotor to the flight model, because the power demanded by maneuvering depends on them [9].

> **TECHNOLOGY** **Final Element: Electric Motors on the Rotors**
>
> A small multirotor needs no mechanical linkage at its rotors. Brushless direct-current motors with electronic speed controllers turn fixed-pitch rotors, and the vehicle is controlled by varying motor speed alone [8]. At air-taxi size the choice is open. Rotor speed control gives a lower design weight, but quadrotors sized for it were found not stabilizable with adequate closed-loop performance within the mechanical limits of their drive systems, and a later solution left the motor current unbounded [9]. A six-passenger helicopter concept for air taxis chose blade pitch control for control bandwidth and for autorotation [21]. The chapter folds motors, rotors and either kind of control into one lag of 0.12 s per rotor group.

Where the Controller Runs

The research quadrotor split its computing into two levels. A microcontroller ran the real-time control loops and wrote the motor commands, while a single-board computer above it ran planning, estimation and position control, with satellite fixes arriving at 10 Hz [8]. The flight computer of this chapter runs all three loops every 10 ms on navigation states delivered at 100 Hz. Its altitude and position loops are velocity-form PID blocks (Section 1.6.2), the tilt loop a PD block with the trim fed forward, and the supervisor a layer above them that sets the targets. The six-passenger concept flown in a motion simulator nested a fast inner attitude loop under an outer loop that shaped the commands [9], the same order of loops.

What Is Modernizing It

Three developments bear on the chapter's question of what the controller knows. The first is onboard weight and balance systems, which measure the actual weight and center of gravity instead of

assuming them [22], the measured counterpart of the load sheet that the payload-aware mode reads. The second is statistical models of satellite errors measured in real street canyons, the groundwork for navigation filters that know how far to trust a fix [20]. The third is predictive control: the six-passenger concept's flight control was a discrete-time model predictive controller whose cost weights set its disturbance rejection [9]. The observer of Section 3.4 belongs to a family of methods that estimate a lumped disturbance and cancel it, applied across industrial sectors for four decades [2].

IN PRACTICE **Where the Load Sheet Gets Its Weights**

United States guidance on weight and balance control names three ways to weigh passengers and bags: standard average weights, averages from the operator's own survey, and actual weights. Standard averages add 5 pounds of clothing in summer and 10 in winter to body weights from health surveys. A small sample strays further from the average, and the guidance limits standard averages to multiengine turbine aircraft with five or more passenger seats. An onboard system that measures the actual weight and center of gravity removes the margins kept for assumed passenger weights, though not the load manifest [22]. A two-seat taxi has far fewer seats, and case 4 shows what a sheet 20 % light costs it.

3.8 Limitations

The model is not a flight model of any aircraft, and its numbers carry no claim about a real air taxi's performance, energy or landing precision. Planar flight removes roll, yaw and their coupling, the rotors lack inflow, flapping and H-force, and the wind field is a set of closed-form features rather than a solution of the flow [6, 12]. The payload-aware modes read a load sheet instead of estimating mass online, and the observer estimates forces, not the wind itself. The dispatch rule is applied on the pad and through the saturation divert, not at the approach gate. The touchdown-speed criterion of the graded route is passed narrowly. Where each assumption breaks is stated in Section 3.3.

OPEN CHALLENGE **Holding Height With Rotor Speed Alone**

The first piloted handling-qualities study of an air-taxi quadrotor in a motion simulator, flown in 2021, compared blade pitch control with rotor speed control. Pilot ratings varied strongly with the standard applied, with the tuning and with turbulence, and turbulence amplified the challenge. The authors note that minimal data exist for large rotor speed-controlled vehicles outside of software, and they set out to measure what disturbance rejection costs in motor power [9]. Progress would be flight data and criteria that fix how much motor power a passenger multirotor needs to hold its height in a gust.

3.9 Conclusion

This chapter studied a drone taxi simulator whose experimental variable is what the flight controller knows. Its nine-state planar multirotor has rotor arms about the true center of mass, a sagging battery limit and a closed-form wind field of shelter, a gap jet, roof-edge flows and wakes, and three loops close at 100 Hz under a supervisor. Fixed tuning holds a light climb within 0.09 m and lets a heavy one fall 1.78 m behind, and correcting the feedforward alone brings it to 0.05 m whether or not the gain is scheduled. A suitcase at the end of the tray costs 2.46° of standing tilt error against a predicted 2.45°. An observer with a 0.67 s time constant cuts the drift after a wind step from 1.19 to 0.36 m and the landing error at the gap's jet from 0.71 to 0.18 m, and on the graded route it alone meets the target, on all 20 seeds tested. A battery at 17 % leaves a full load a margin of 22.4 %, and the supervisor holds on the pad. The field is illustrative, flight is planar and the rotors have no inflow dynamics. A fuller model would add an online mass estimate, out-of-plane wind, rotor inflow and a predictive controller that plans the approach within the tilt and thrust limits.

The drone taxi is a study in giving a feedback loop the knowledge it cannot learn fast enough from its own error.

KEY POINTS

- A loop not told its load carries the extra weight only through its error, so fixed tuning lets a heavy climb fall 1.78 m behind.
- Correcting the weight feedforward alone brings that climb to 0.05 m whether or not the gain is scheduled: the feedforward does the work.
- The tilt loop has no integral, so a suitcase at the end of the tray costs 2.46° of standing tilt error against a predicted 2.45°.
- An observer with a 0.67 s time constant cuts the drift after a wind step from 1.19 to 0.36 m, and on the graded route it alone meets the target, on all 20 seeds tested.

Where else this applies. Chapter 6 carries wind and current as a slowly varying force that its observer feeds forward, and the climber of Volume 3, Chapter 12 feeds forward a weight that changes along its route.

References

[1] K. Ohishi, M. Nakao, K. Ohnishi, and K. Miyachi, "Microprocessor-controlled DC motor for load-insensitive position servo system," *IEEE Transactions on Industrial Electronics*, vol. IE-34, no. 1, pp. 44–49, 1987.

[2] W.-H. Chen, J. Yang, L. Guo, and S. Li, "Disturbance-observer-based control and related methods—an overview," *IEEE Transactions on Industrial Electronics*, vol. 63, no. 2, pp. 1083–1095, 2016.

[3] W. J. Rugh and J. S. Shamma, "Research on gain scheduling," *Automatica*, vol. 36, no. 10, pp. 1401–1425, 2000.

[4] R. Mahony, V. Kumar, and P. Corke, "Multirotor aerial vehicles: Modeling, estimation, and control of quadrotor," *IEEE Robotics & Automation Magazine*, vol. 19, no. 3, pp. 20–32, 2012.

[5] A. Bacchini and E. Cestino, "Electric VTOL configurations comparison," *Aerospace*, vol. 6, no. 3, p. 26, 2019.

[6] I. P. Castro and A. G. Robins, "The flow around a surface-mounted cube in uniform and turbulent streams," *Journal of Fluid Mechanics*, vol. 79, no. 2, pp. 307–335, 1977.

[7] D. Galway, J. Etele, and G. Fusina, "Modeling of urban wind field effects on unmanned rotorcraft flight," *Journal of Aircraft*, vol. 48, no. 5, pp. 1613–1620, 2011.

[8] G. Hoffmann, H. Huang, S. Waslander, and C. Tomlin, "Quadrotor helicopter flight dynamics and control: Theory and experiment," in *AIAA Guidance, Navigation and Control Conference and Exhibit*. American Institute of Aeronautics and Astronautics, 2007.

[9] S. Withrow-Maser, J. Aires, A. Ruan, C. Malpica, and S. Schuet, "Evaluation of heave disturbance rejection and control response criteria on the handling qualities evaluation of urban air mobility (UAM) eVTOL quadrotors using the vertical motion simulator," in *Vertical Flight Society Aeromechanics for Advanced Vertical Flight Technical Meeting*, San Jose, CA, 2022, nASA Technical Reports Server 20210026423, https://ntrs.nasa.gov/citations/20210026423.

[10] B. W. Bequette, "Process control practice and education: Past, present and future," *Computers & Chemical Engineering*, vol. 128, pp. 538–556, 2019.

[11] J. A. Rossiter, B. Pasik-Duncan, S. Dormido, L. Vlacic, B. Jones, and R. Murray, "A survey of good practice in control education," *European Journal of Engineering Education*, vol. 43, no. 6, pp. 801–823, 2018.

[12] W. Johnson, *Rotorcraft Aeromechanics*. Cambridge University Press, 2013.

[13] R. W. Prouty and H. C. Curtiss, Jr., "Helicopter control systems: A history," *Journal of Guidance, Control, and Dynamics*, vol. 26, no. 1, pp. 12–18, 2003.

[14] T. Tomic, C. Ott, and S. Haddadin, "External wrench estimation, collision detection, and reflex reaction for flying robots," *IEEE Transactions on Robotics*, vol. 33, no. 6, pp. 1467–1482, 2017.

[15] S. Watkins, J. Burry, A. Mohamed, M. Marino, S. Prudden, A. Fisher, N. Kloet, T. Jakobi, and R. Clothier, "Ten questions concerning the use of drones in urban environments," *Building and Environment*, vol. 167, p. 106458, 2020.

[16] A. Straubinger, R. Rothfeld, M. Shamiyeh, K.-D. Büchter, J. Kaiser, and K. O. Plötner, "An overview of current research and developments in urban air mobility – setting the scene for UAM introduction," *Journal of Air Transport Management*, vol. 87, p. 101852, 2020.

[17] W. L. Fredericks, S. Sripad, G. C. Bower, and V. Viswanathan, "Performance metrics required of next-generation batteries to electrify vertical takeoff and landing (VTOL) aircraft," *ACS Energy Letters*, vol. 3, no. 12, pp. 2989–2994, 2018.

[18] L. L. Hoberock, "A survey of longitudinal acceleration comfort studies in ground transportation vehicles," *Journal of Dynamic Systems, Measurement, and Control*, vol. 99, no. 2, pp. 76–84, 1977.

[19] T. Kroger and F. M. Wahl, "Online trajectory generation: Basic concepts for instantaneous reactions to unforeseen events," *IEEE Transactions on Robotics*, vol. 26, no. 1, pp. 94–111, 2010.

[20] M. Peretic, R. Gilabert, J. Carroll, J. Gutierrez, A. Moore, J. Christie, and E. T. Dill, "Statistical analysis of GNSS multipath errors in urban canyons," in *IEEE/ION Position, Location and Navigation Symposium (PLANS)*, Salt Lake City, UT, 2025, nASA Technical Reports Server 20250000589, https://ntrs.nasa.gov/citations/20250000589.

[21] W. Johnson, C. Silva, and E. Solis, "Concept vehicles for VTOL air taxi operations," in *AHS Technical Conference on Aeromechanics Design for Transformative Vertical Flight*, San Francisco, CA, 2018, nASA Technical Reports Server 20180003381, https://ntrs.nasa.gov/citations/20180003381.

[22] Federal Aviation Administration, "Aircraft weight and balance control," Advisory Circular 120-27F, 6 May 2019, https://www.faa.gov/documentLibrary/media/Advisory_Circular/AC_120-27F.pdf, 2019.

3.10 Exercises

3.1 Concept check · 2 min

In the steady hover of scenario 1 with the 40 kg suitcase of case 5 at the left end of the tray, the fixed tuning holds a tilt error of 2.46° for as long as the vehicle hovers. Why does the error not decay?

(a) The tilt loop has no integral action, so a standing moment needs a standing error
(b) The position loop's integral keeps moving the tilt setpoint away from the tilt
(c) The 0.12 s thrust lag delays every correction beyond the length of the hover
(d) The tilt measurement noise hides an error smaller than its standard deviation

3.2 Concept check · 2 min

In case 4 the load sheet is 20 % light. With the observer added, the vehicle still lifts off 1.17 s after the climb begins, as late as the payload-aware mode without it. Why does the observer not help at liftoff?

(a) Its bandwidth of 1.5 rad/s is too slow to act within 1.17 s
(b) It is reset to zero on the ground, and a weight the pad carries causes no motion to estimate
(c) It estimates only the horizontal force, so a weight error is outside its reach
(d) The dispatch rule holds the vehicle on the pad until the estimate has settled

3.3 Concept check · 2 min

With the fixed tuning, the heavy climb of case 3 falls 1.78 m behind its reference. Which single change brings it within about 0.05 m?

(a) Scheduling the altitude gain on the true mass while keeping the 480 kg weight feedforward
(b) Halving the altitude integral time, so that the integral catches up faster
(c) Setting the design mass to 620 kg, which corrects the weight feedforward at the same gain
(d) Raising the observer bandwidth to 4 rad/s with the fixed controller still selected

3.4 Theory and calculation · 6 min

Case 5 boards one 80 kg passenger and a 40 kg suitcase at $x_b = -1.5$ m on the 400 kg vehicle, with $\ell = 2.0$ m and $g = 9.81\,\mathrm{m/s^2}$.

(a) Use Equation (3.3) to find the mass and the center of mass c. *Checkpoint:* 520 kg and −11.5 cm.

(b) Find the differential thrust $T_R - T_L$ that holds a level hover. *Checkpoint:* −294 N.

(c) The fixed tuning feeds no trim forward and its tilt gain is 120 N/°. Predict the standing tilt error, to two decimals. *Checkpoint:* 2.45°.

3.5 Theory and calculation · 7 min

Use the error budget of Section 3.5 with $g = 9.81\,\mathrm{m/s^2}$.

(a) In case 3 the fixed tuning believes 480 kg and the heavy leg weighs 620 kg, with an altitude gain of 700 N/m. Find the unknown force and the proportional-only error e_P. *Checkpoint:* 1.37 kN and 1.96 m.

(b) In case 4 the payload-aware mode reads a load sheet 20 % light on the same 620 kg and schedules its gain as $K_{c,z}\hat{m}/m_{nom}$ with $K_{c,z} = 700\,\mathrm{N/m}$ and $m_{nom} = 480\,\mathrm{kg}$. Find $\hat{m}$, the unknown force, the scheduled gain and e_P. *Checkpoint:* 496 kg, 1.22 kN, 723 N/m, 1.68 m.

(c) The observer has $K = 1.5\,\mathrm{rad/s}$. How long does its estimate of a step force take to reach 63 % and 95 % of the force? *Checkpoint:* 0.67 s and 2.0 s.

3.6 Theory and calculation · 8 min

Case 9 starts at a charge of $s = 0.17$. The battery has $P_{max} = 190\,\mathrm{kW}$, a sag knee $s_k = 0.35$, power at empty $p_f = 0.5$ and avionics power $P_{av} = 1.5\,\mathrm{kW}$. Each rotor group has $A = 12\,\mathrm{m}^2$ and $FM = 0.6$ in air of $1.225\,\mathrm{kg/m}^3$, and $g = 9.81\,\mathrm{m/s}^2$.

(a) Use Equation (3.6) to find $f(s)$ and the thrust one group can deliver. *Checkpoint:* 0.743 and 3.72 kN.

(b) Find the thrust margin μ for the full load of 620 kg, and the supervisor's decision under the 25 % rule. *Checkpoint:* 22.4 %, hold on the pad.

(c) Find the margin with one 100 kg passenger off, and the margin the fixed mode computes for the full load from its 480 kg design mass. *Checkpoint:* 46.0 % and 58.1 %, each within 0.2 %.

3.7 App challenge · 8 min

Load scenario 3, Light versus full load, with the default seed. A playback speed of 2 suits each run.

(a) Run to 66 s as loaded, with the Fixed controller, and export the CSV file. For each of the two climbs, the rows whose `phase` is `climb`, find the largest value of `z_sp_m` − `z_m`. *Checkpoint:* 0.08 m and 1.75 m, each within 0.03 m.

(b) Press Reset, set Controller to Payload-aware before Run, run to 66 s again and find the same value for the second climb. *Checkpoint:* 0.05 m, within 0.01 m.

(c) Compare part (a) with the proportional-only error of Table 3.5, and say which of the two changes the payload-aware mode makes, the weight feedforward or the scheduled gain, removes the lag. *Checkpoint:* 1.96 m predicted, and the feedforward.

3.8 App challenge · 8 min

Load scenario 6, Steady crosswind, with the default seed. The wind steps from calm to 8 m/s at 5 s. Each run lasts 30 s. Read the `x_m` and `x_sp_m` columns of the exported CSV file.

(a) Run as loaded, with the Payload-aware controller. Find the largest $|$`x_m` − `x_sp_m`$|$ after 5 s, the time of that row, and the first later row in which the distance is under 0.1 m. *Checkpoint:* 1.19 m at 12.25 s, back at 24.65 s, each time within 0.1 s.

(b) Press Reset, set Controller to + wind estimate before Run, and repeat. *Checkpoint:* 0.36 m at 7.70 s, back at 13.30 s.

(c) Press Reset, also set Observer bandwidth to 4.0 before Run, and read the largest distance again. Name the price of the faster estimate, using the bandwidth sweep of Section 3.6. *Checkpoint:* 0.24 m, within 0.01 m.

3.9 App challenge · 9 min

Load the challenge, the afternoon route, with the default seed, and use a playback speed of 5. Each run ends by itself about 135 s after Run, when the route is complete. Read the Touchdowns in spec and Battery reserve tiles of the scorecard after each run.

(a) Run as loaded, with the Fixed controller. *Checkpoint:* 1 of 2, worst 0.45 m/s and 0.99 m, 22.5 %.

(b) Press Reset, set Controller to Payload-aware before Run, and run again. *Checkpoint:* 1 of 2, worst 0.45 m/s and 0.98 m, 22.4 %.

(c) Press Reset, set Controller to + wind estimate before Run, and run again. Explain why only this run passes. *Checkpoint:* 2 of 2, worst 0.41 m/s and 0.23 m, 22.6 %.

3.10 Application area · 4 min

Case 2 flies the same hop twice. As shipped it takes 35.3 s from liftoff to touchdown and uses 0.76 kWh. With gentle limits of 1.2 m/s^2 and 1.0 m/s^3 it takes 43.2 s and uses 0.92 kWh. The vehicle weighs 490 kg and hovers on 73.9 kW.

(a) Estimate the extra energy of the gentle hop from the hover power and the extra time aloft, and compare it with the measured difference. *Checkpoint:* 0.162 kWh against 0.16 kWh.

(b) An operator wants the gentle limits for passenger comfort on every hop. Name two things the operator must budget for, and why a ground vehicle pays far less for the same choice. *Checkpoint:* Trip time and battery energy. A car does not spend power to stay up.

3.11 Application area · 3 min

Aviation load control often uses standard passenger masses. Case 4 shows a load sheet 20 % light on a vehicle of 620 kg.

(a) How much mass and weight does the sheet miss, with $g = 9.81\,\mathrm{m/s^2}$? *Checkpoint:* 124 kg and 1.22 kN.

(b) Give two reasons an underestimate is the dangerous direction for this vehicle, one in the loops and one in the supervisor. *Checkpoint:* A late liftoff and a lag, and a dispatch margin that reads too high.

3.12 Review the agent · 5 min

A student asks an AI assistant what happens in case 5 when the suitcase slides from the left to the right end of the tray in flight, with Controller set to + wind estimate. The assistant replies: “The disturbance observer estimates whatever the load sheet missed. It will see the shifted center of mass and remove the tilt error within a couple of seconds, about three of its time constants of 0.67 s.” Find the flaw and say how you would check it.